An RF-based System for Tracking Transceiver-free Objects

Dian Zhang, Jian Ma, Quanbin Chen, and Lionel M. Ni
Department of Computer Science and Engineering
Hong Kong University of Science and Technology
Clear Water Bay, Kowloon, Hong Kong
{zhangd,majian,chenqb,ni}@cse.ust.hk

Abstract

In traditional radio-based localization methods, the target object has to carry a transmitter (e.g., active RFID), a receiver (e.g., 802.11x detector), or a transceiver (e.g., sensor node). However, in some applications, such as safe guard systems, it is not possible to meet this precondition. In this paper, we propose a model of signal dynamics to allow tracking of transceiver-free objects. Based on Radio Signal Strength Indicator (RSSI), which is readily available in wireless communication, three tracking algorithms are proposed to eliminate noise behaviors and improve accuracy. The midpoint and intersection algorithms can be applied to track a single object without calibration, while the best-cover algorithm has potential to track multiple objects but requires calibration. Our experimental test-bed is a grid sensor array based on MICA2 sensor nodes. The experimental results show that the best side length between sensor nodes in the grid is 2 meters and the best-cover algorithm can reach localization accuracy to 0.99m.

1. Introduction

Real-time tracking of moving objects is highly in demand and important to many applications, such as vehicle tracking [2], battlefield surveillance [18], animal habitat monitoring [25], and patient tracking in hospitals [5]. It has attracted a great deal of attention in various research communities. GPS [21] is a technology well known for its accuracy. However, GPS only works in outdoor environments without satellite signals being blocked. Moving object tracking in indoor environments is more complicated and several technologies, such as video, pressure, infrared, and ultrasound, have been proposed. These technologies are usually costly, including infrastructure, deployment, and maintenance, and may have some restrictions placed on the environments in which they are applied. For example, video technology based on real-time image processing is a feasible solution. However, video technology does not work in dark environments and the privacy of those being tracked creates another concern.

Radio frequency (RF) is another promising technology, which utilizes *Radio Signal Strength Indicator* (RSSI) to track moving objects if both moving objects and some reference objects are using RF signals to communicate. In theory, the RSSI obtained by the receiver is a function of the distance between the transmitter and the receiver as indicated in many propagation models [16]. However, in practice, there are many problems in applying these models. The indoor layout structure, objects, and humans can cause reflection, refraction, diffraction, and absorption of radio signals. Therefore, severe multi-path phenomenon will occur and affect the accuracy of indoor location sensing. Moreover, many other factors also influence the RSSI, such as temperature, orientation of antenna, and height to the ground [7]. Nevertheless, since RSSI is readily available in wireless communication without additional cost, RF-based localization has become a hot research issue in wireless networks [3] [10] [11] [13] [25].

In RF-based localization, both target objects and reference objects have to communicate with others to collect RSSI information for location estimation. There are three basic models. In the first model, the target object has to carry a transmitter (e.g., active RFID tags) to periodically transmit beacon messages (e.g., the ID of the RFID tag). Many receivers (e.g., RFID readers) with known locations may measure the RSSI values of received beacon messages and cooperate to estimate the locations of the target objects. In the second model, the target object has to carry a receiver (e.g., 802.11x detectors). The target object is able to receive RSSI information from nearby transmitters (e.g., 802.11x access points) and estimate its current location. In the third model, each object has a transceiver (e.g., sensor nodes) and exchange information with other objects. Based on the RSSI information

Proceedings of the Fifth Annual IEEE International
Conference on Pervasive Computing and Communications (PerCom'07)
0-7695-2787-6/07 $20.00 © 2007 IEEE

collected from nearby objects, the target object may be able to estimate its location. In order to improve the localization accuracy, many techniques have been proposed and this subject remains a hot research issue.

In the above three models, the target object has to carry a transmitter, a receiver, or a transceiver. This precondition, however, cannot be met in some applications, such as safe guard systems. The objective of this paper is to investigate if the location of moving objects can be estimated without carrying any RF device in an environment covered by a wireless sensor network (WSN) where sensor nodes exchange information with each other[1]. To the best of our knowledge, this is the first paper that attempts to track transceiver-free objects using RF-based technology. Our initial research shows that this is possible using some novel approaches as described later.

The basic idea of this paper is to construct a signal dynamic model to obtain the property of the RSSI changing behaviors in WSNs. Based on this model and its property, we propose three tracking algorithms: midpoint algorithm, intersection algorithm, and best-cover algorithm. Through using these algorithms, we can eliminate the noise behaviors and improve tracking accuracy. The midpoint and intersection algorithms can be applied to track a single object without calibration, while the best-cover algorithm has potential to track multiple objects but requires calibration.

Our experimental test-bed is a grid sensor array based on MICA2 sensor nodes [23]. The experimental results show that the best side length between sensor nodes in the grid is 2 meters and the best-cover algorithm can reach localization accuracy to 0.99m. In real-time moving object experiments, the tracking latency is about three seconds, which is dependent on the information exchange interval between sensor nodes. The best-cover algorithm can also recognize multiple objects if these objects are not tightly close to each other. In short, the best-cover algorithm can perform transceiver-free object tracking as long as the objects are not crowded in an area covered by a well-structured WSN.

The rest of this paper is organized as follows. In the next section, we provide some related work and give a comparative overview. Section 3 introduces the signal dynamic model and the associated property. The proposed three tracking algorithms are described in Section 4. We then show the experimental results and evaluate the performance in Section 5. Lastly, we conclude the paper and list our future work.

[1] In fact, we only take advantage of the communication behavior of sensor nodes, not the associated sensing device.

2. Related Work

Other than the RF technology, some other technologies might be used to track moving objects.

Video. In the computer vision area, by applying many video-based algorithms on sequences of images from a camera or synchronized images captured from multiple cameras, moving people can be tracked [4] or the number of people in a certain area can be counted [22]. However, this technology is expensive and fails in darkness. Moreover, it may violate the privacy of people.

Infrared. In the context of infrared wireless networks, the limited range of an infrared network, which facilitates the user location, is a handicap in providing ubiquitous coverage. For example, some companies, such as Acorel [1], already have some products based on infrared technology. However, they can only record how many people enter or exist in a restricted area by monitoring that area's access, such as the door of a room. Moreover, this technology requires careful and dense deployment, and does not work in a more complicated environment.

Pressure. An optional localization technology is to use acceleration and air pressure sensors to detect people's footsteps [17]. The obvious drawbacks of this technology are the high cost and need for careful deployment.

Ultrasound. The technologies using ultrasonic sensor networks usually require the target object to carry a transmitter or receiver. Most of them adopt an ultrasonic Time-Of-Flight (TOF) method to obtain location information. For example, in the Bat Ultrasonic Location System [19], the target object must carry a Bat (transmitter), while this Bat periodically emits a short pulse of ultrasound. The Cricket Location-Support System [15] uses a combination of ultrasound and RF to provide a location-support service. It allows applications running on mobile and static nodes to learn their physical locations by using listeners (receivers) that hear and analyze information from beacons spread throughout the building.

As mentioned earlier, three indoor localization models have been studied using the RF technology. They are 802.11, active RFID, and wireless sensor networks.

802.11. 802.11 technologies use a standard network adapter to measure signal strengths. This approach utilizes signal strength information gathered from known multiple access points to locate objects. Some approaches build a radio map of signal strength value for each location [3] [24]. All these methods need the target object to carry a radio detector (receiver).

RFID. LANDMARC can localize the target object

Proceedings of the Fifth Annual IEEE International
Conference on Pervasive Computing and Communications (PerCom'07)
0-7695-2787-6/07 $20.00 © 2007 IEEE

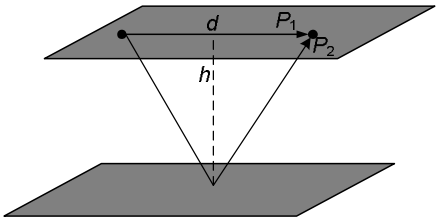

Figure 1: Static environment

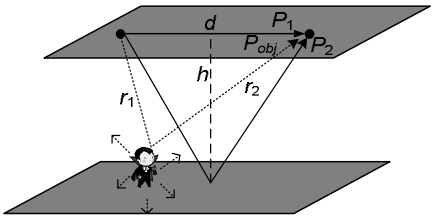

Figure 2: Dynamic environment

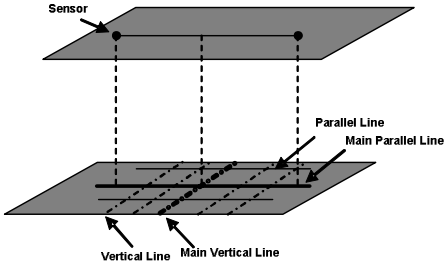

Figure 3: Position classification on the ground

carrying an active RFID [11]. It adopts a number of reference tags to alleviate the fluctuation feature in RSSI and then utilizes K nearest reference tags' coordinates to compute the coordinate value of the tracking tag. However, this method also requires the target object to carry a tracking tag, which is an active RFID (transmitter). In addition, the RFID readers are expensive. Therefore, it will cost much if applied to a large area. Our system only uses the cheaper MICA2 sensor nodes [23].

Wireless Sensor Networks. Similarly, in RF-based WSNs, the information gathered from sensors is used to infer the global or application-defined local coordinates of the objects. Most of the object localization methods calculate distance or count the hop number to some nodes whose positions are already known, or measure the angle of arrival to derive location information [8] [9] [10] [12] [13] [25]. The target object also has to carry a sensor node (transceiver) to send or receive the packets.

3. The Signal Dynamic Model

We have to understand how the movement of an object will affect the signal strength of two communicating sensor nodes. To focus on this effect, we consider a *static environment*, shown in Figure 1, where two sensor nodes are fixed on the ceiling with d distance apart and are h distance from the ground. For the corresponding *dynamic environment*, shown in Figure 2, at least one object moves in the environment. All other factors, such as temperature, remain unchanged.

3.1. Theoretical background

In an indoor static environment, there should be two main radio propagation paths between the transmitter and the receiver besides the multi-path reflections of the surroundings. One is the line-of-sight path and the other is the ground reflection path as illustrated in Figure 1.

For the direct line-of-sight propagation path, according to the free space model, the power received by the receiver is given by the Friis free space equation [16] as

$$P_1 = \frac{P_t G_t G_r \lambda^2}{(4\pi)^2 d^2} \quad (1)$$

where P_t is the transmitted power in watts, P_1 is the received power in watts, G_t is the transmitter antenna gain, G_r is the receiver antenna gain, λ is the wavelength in meters, and d is the distance from transmitter to receiver.

For the ground reflection path, the power received by the receiver can be expressed as

$$P_2 = \frac{P_t G_t G_r \lambda^2}{(4\pi)^2 (d^2 + 4h^2)} \quad (2)$$

Suppose the intensity magnitudes of the line-of-sight path and the ground reflection path are E_1 and E_2, respectively. E_{other} is the intensity magnitude of other radio propagation paths, such as the reflections of the surroundings. The total received power by the receiver P_0 in the indoor static environment is expressed below.

$$P_0 \propto |E_1 + E_2 + E_{other}|^2 \quad (3)$$

This value is almost stable in a static environment although noise does exist.

When a finite-sized object comes into this static environment, the target object will scatter the incident power in various directions as illustrated in Figure 2. According to radar equation [14], the received power influenced by the target is

$$P_{obj} = \frac{P_t G_t G_r \lambda^2 \sigma}{(4\pi)^3 r_1^2 r_2^2} \quad (4)$$

where r_1 is the distance from the transmitter to the target object, r_2 is the distance from the target object to the receiver, and σ is the radar cross section of the target object. The radar cross section σ is defined as the ratio of scattered power to incident power density.

According to scattering theory [6], in the dynamic environment, E_1, E_2 and E_{other} will not change their values. The total received power by the receiver is the sum of incident and scatted waves as below

$$P \propto |E_1 + E_2 + E_{other} + E_{obj}|^2 \quad (5)$$

where E_{obj} is the intensity magnitude of scatted wave

Proceedings of the Fifth Annual IEEE International
Conference on Pervasive Computing and Communications (PerCom'07)
0-7695-2787-6/07 $20.00 © 2007 IEEE

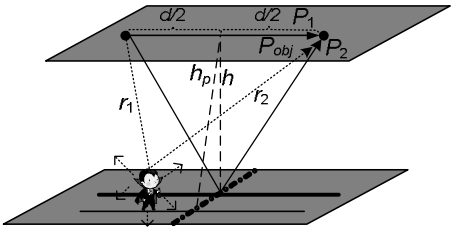

Figure 4: Proof of the signal dynamic property

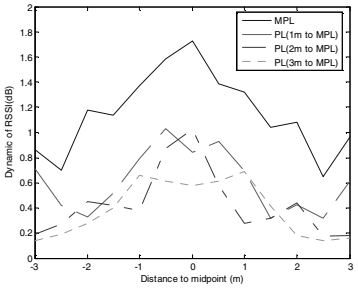

Figure 5: PL view of model test

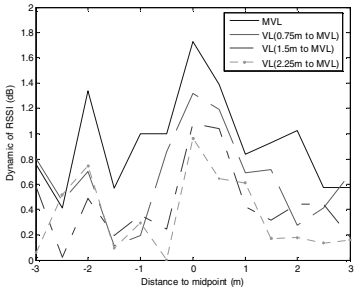

Figure 6: VL view of model test

caused by the target object.

Based on Eqs. [1-5], as long as $P_{obj} << P_{0,}$ we get the difference of power received by the receiver as below.

$$\Delta P \approx P_{obj} \qquad (6)$$

That is, if the condition $P_{obj} << P_0$ is satisfied, the difference of signal strength between static environment and dynamic environment is approximately proportional to P_{obj}. Here we omit the proof part because of the page limitation.

3.2. Signal dynamic property

At first, we classify the object position on the ground as shown in Figure 3. The *main parallel line* (MPL) is the mapping on the ground of the transmitter-receiver. The *main vertical line* (MVL) is perpendicular to MPL crossing the midpoint of MPL. *Parallel Lines* (PL) and *Vertical Lines* (VL) are on the ground and parallel or equal to MPL and MVL, respectively. Second, suppose we have m number of RSSI values in the static environment, which are a_1, a_2, …, a_m and b is the RSSI value in the dynamic environment. We define the *RSSI dynamic* as below.

$$\frac{\sum_{i=1}^{m} |b - a_i|}{m}$$

Based on the theoretical background, we have the following property to describe the signal dynamics.

Signal dynamic property: *Along each PL or VL, if the object position is closer to its midpoint, the RSSI dynamics caused by the object are larger*.

Let us verify the signal dynamic property. First, suppose the object is on one PL as shown in Figure 4. We define h_p as the distance between the midpoint of the PL and the midpoint of the transmitter-receiver, and x as the distance between the object and the midpoint of the PL. The deduction is as follows.

$$r_1^2 = \left(x - \frac{d}{2}\right)^2 + h_p^2 \quad , \quad r_2^2 = \left(x + \frac{d}{2}\right)^2 + h_p^2$$

$$\begin{aligned} r_1^2 r_2^2 &= \left(\left(x - \frac{d}{2}\right)^2 + h_p^2\right)\left(\left(x + \frac{d}{2}\right)^2 + h_p^2\right) \\ &= x^4 + 2(h_p^2 - \frac{d^2}{4})x^2 + \left(\frac{d^2}{4} + h_p^2\right)^2 \\ &= \left(x^2 + h_p^2 - \frac{d^2}{4}\right)^2 + h_p^2 d^2 \end{aligned}$$

When x becomes smaller, the value of $r_1^2 r_2^2$ also grows smaller. According to Eqs. (4) and (6), P_{obj} is inverse proportional to $r_1^2 r_2^2$. We prove that along each PL, when the object is closer to its midpoint, P_{obj} is larger.

Suppose the object position is on one VL. Because the midpoint of each VL is on MPL, the line from the transmitter or receiver to the midpoint of VL is perpendicular to the VL. Thus, the value of $r_1^2 r_2^2$ becomes smaller when the object moves closer to its midpoint. We prove that along each VL, if the object is closer to the midpoint of it, P_{obj} is larger.

Based on Eqs. (6), the difference of signal strength between static environment and dynamic environment is approximately proportional to P_{obj}. Therefore, the signal dynamic property is verified.

3.3. Experimental verification of the model

In order to verify the signal dynamic property further, we use two MICA2 sensor nodes [23]. Its detail setting is described in the next section. Each sensor acts as both a transmitter and a receiver. These two sensor nodes are placed 3m apart on the ceiling of a room with the height of 2.4m. We arrange one person to act as the target object and test different PL and VL positions.

We show the relationship between the positions of the person and the related RSSI dynamics from the PL direction and VL direction in Figure 5 and Figure 6, respectively. The coordinates of the two sensors are (0, -1.5) and (0, 1.5), respectively. For each PL and each VL, we find that the RSSI dynamics bump up around the center (0, 0). That is, the person standing at the

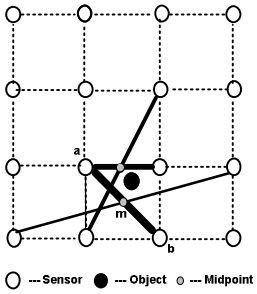

Figure 7: An example of mid-points algorithm

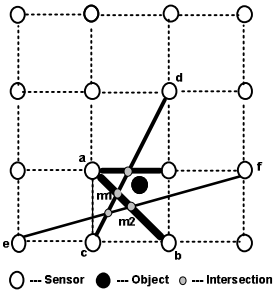

Figure 8: An example of intersection algorithm

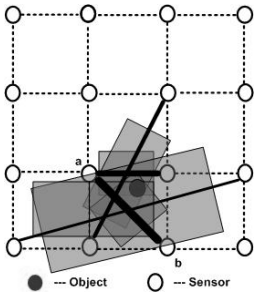

Figure 9: An example of best-cover algorithm

midpoint of MPL or MVL has the largest RSSI dynamics. For each PL or each VL, although there are some fluctuations at some positions due to noise behavior, in general, the RSSI dynamics are larger as the person moves closer to its midpoint. We also observe that when the object position is on the MPL or MVL, the RSSI dynamics are much larger than it is when the person is at the same place on the other PLs or VLs.

From our experiments, we further verified that the relationship between the person-position and the associated RSSI dynamics does obey the signal dynamic property.

4. Methodology

Extending our signal dynamic model, we deploy sensors in a regular 2D grid array, in which the positions of all the nodes are predetermined. Each node broadcasts beacon messages periodically and listens to the beacons from its neighbors as well.

The basic idea of our methodology is to detect the RSSI dynamics due to the movement of objects. Because noise behavior sometimes can also generate some RSSI dynamics, in order to reduce the influence of noise, we set a *dynamic threshold* for each wireless link. Only when the measured RSSI dynamics on a link is larger than its threshold, we call the link as an *influential link*. Based on the signal dynamic property, the influential links tend to cluster around the object position. Thus, we can employ these influential links to locate the target objects.

In this section, first we present the midpoint and intersection algorithms, which can be applied to track a single object without calibration. Then, in order to improve the accuracy and track multiple objects, we propose the best-cover algorithm, which requires calibration on the wireless links with the same distance.

4.1. Midpoint algorithm

Based on our model, by using the sensor grid, the influential links tend to cluster around the object. The midpoint algorithm utilizes the midpoints of the influential links to estimate the object location. We assign a weight value to the midpoint of each influential link according to its RSSI dynamic value. The object position can be calculated as the weighted average of these midpoints' positions.

An example is illustrated in Figure 7, where a thicker influential link implies that it has a larger RSSI dynamic value. For example, link *ab* is one of the influential links. *m* is the midpoint of link *ab*. From the signal dynamic property, link *ab* having a larger RSSI dynamic value means it is closer to the object position, so is the midpoint *m* of link *ab*. In this example, there are four midpoints on four influential links (some of them are overlapped).

Since the coordinates of all the sensor nodes are known in advance, for each influential link, the midpoint coordinate (x_i, y_i) can be calculated. The weight of each influential link is p_i, which is the RSSI dynamic value of the link. Assuming we have in total n influential links, we compute the weighted average of all the midpoints and get the object position coordinate value (x_{obj}, y_{obj}) as below.

$$x_{obj} = \frac{\sum_{i=1}^{n} p_i \cdot x_i}{\sum_{i=1}^{n} p_i}, \quad y_{obj} = \frac{\sum_{i=1}^{n} p_i \cdot y_i}{\sum_{i=1}^{n} p_i}$$

Since we only need to compute the midpoint coordinate of each influential link, the complexity of the midpoint algorithm is $O(n)$, where n is the number of influential links.

4.2. Intersection algorithm

The intersection algorithm improves the midpoint algorithm by using the intersection points of influential links instead of the midpoints of them. This is because more points on the influential links offer more information of the object location. If there are more intersection points, the possibility that the links are caused by noise is smaller. For each intersection point, we assign it a weigh value as the sum of RSSI dynamic

Proceedings of the Fifth Annual IEEE International
Conference on Pervasive Computing and Communications (PerCom'07)
0-7695-2787-6/07 $20.00 © 2007 IEEE

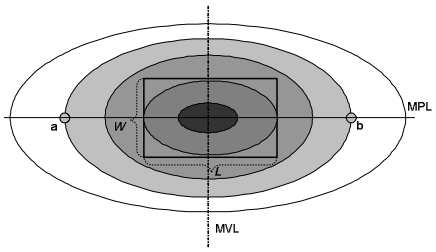

Figure 10: Illustration of one influential link

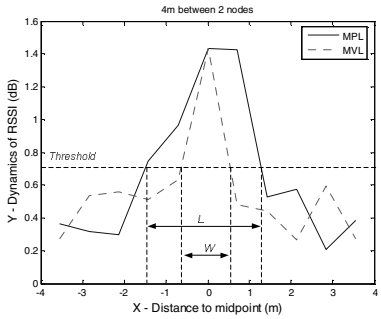

Figure 11: Calibration on sensor distance with 4m

Figure 12: Experimental environment

values of the two crossing links. Then, we average all the intersection points to calculate the object position.

An example is illustrated in Figure 8. Besides the influential link *ab* shown in the same scenario as in Figure 7, links *cd* and *ef* are also influential links. *m*1 *is* the intersection point between link *ab* and link *cd*. *m*2 *is* the intersection point between link *ab* and link *ef*. From the signal dynamic property, if the influential link has a larger RSSI dynamic value, it will be closer to the object position. Therefore, links *ab*, *cd*, and *ef* are all close to the object. Moreover, link *ab* also has intersections with links *cd* and *ef*. The intersection points *m*1 and *m*2 are both close to the object and the possibility that link *ab* is caused by noise is small. Therefore, for link *ab*, instead of using only one midpoint, we utilize two intersection points for the object computation.

Since the coordinates of all nodes are known in advance, we can calculate the intersection coordinate value (x_i, y_i) of any two influential links in advance. Furthermore, the weight p_i of the two intersected influential links is defined as the sum of the RSSI dynamic value of the two influential links.

Suppose the number of influential links is *n* and the number of intersection points is *l*. We calculate the estimated object-position (x_{obj}, y_{obj}) as the weighted average value of all the intersection points.

$$x_{obj} = \frac{\sum_{i=1}^{l} p_i \cdot x_i}{\sum_{i=1}^{l} p_i} \quad , \quad y_{obj} = \frac{\sum_{i=1}^{l} p_i \cdot y_i}{\sum_{i=1}^{l} p_i}$$

Since we need to calculate the intersection coordinate of each two influential links, the total algorithm complexity is $O(n^2)$, where *n* is the number of influential links.

4.3. Best-cover algorithm

Instead of utilizing points on the influential links as described in previous algorithms, for each influential link, the best-cover algorithm creates a rectangle area, in which the object is likely to reside. Therefore, in the sensor grid, there are many rectangles and some of them will overlap as shown in Figure 9. It is obvious that if one place has more overlapping rectangles, the object is more likely to be within that area. Therefore, in this algorithm, we use a square with a fixed area to scan in the grid area. At each scanning position, we calculate the sum of the intersection area between the scanning square and the generated rectangles on each influential link. We also define *covering rate* as the ratio of the number of rectangles intersecting with the scanning square to the total number of rectangles on all the influential links. The most possible object location is the position of the scanning square with the largest total covering area and the calculation reliability is according to its covering rate. Because the scanning square is an estimated area to represent the target object, such as a person, we adopt a square to be 0.5×0.5 square meters in our experiments.

As far as multiple objects are concerned, we define a *cluster* as a collection of rectangles, among which each two rectangles can be connected directly or indirectly by other rectangles. Each cluster represents one object inside so that we can identify the number of objects by counting the number of clusters. For each cluster, we define a *covering area*, which is the sum area of all the associated rectangles. We can eliminate the noise behaviors since a cluster caused by noise usually has a very small covering area. However, if multiple objects are tightly close to each other, we may underestimate the number of objects because their corresponding clusters may merge into one cluster.

Given a pair of sensor nodes, in order to estimate the size of its rectangle area, we should do calibrations before running this algorithm. According to our signal dynamic property, when the object is on MPL or MVL, the RSSI dynamic is much larger than it is when the object is at the same place on other PLs or VLs. Therefore, given an RSSI dynamic value of one influential link, such as link *ab* in Figure 9, the possible area of the object-position is likely covered in an ellipse

Proceedings of the Fifth Annual IEEE International
Conference on Pervasive Computing and Communications (PerCom'07)
0-7695-2787-6/07 $20.00 © 2007 IEEE

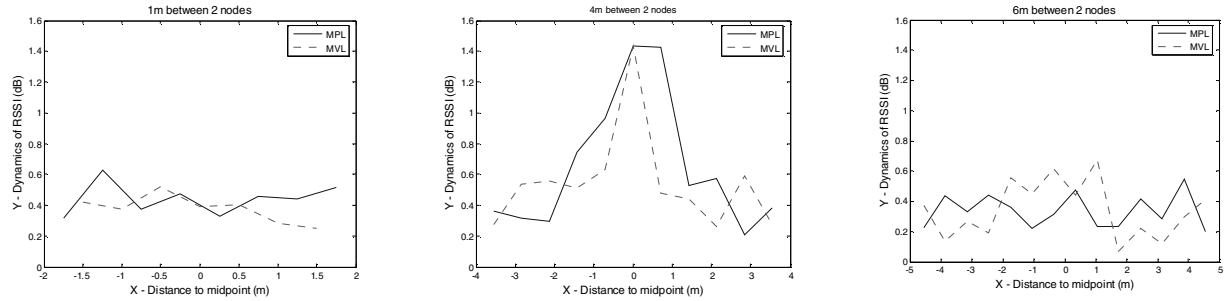

Figure 13: Dynamic behaviors on different sensor distances

shown in Figure 10. To simplify the calculation, we use a bounding rectangle instead of the ellipse to represent this area. Let L and W represent the length and width of the rectangle, respectively. In order to get the related value of L and W of the rectangle on each influential link, we perform the calibration for different sensor distances. For each sensor distance, we arrange a person to stand at different positions of its MPL and MVL, and then we record the related RSSI dynamic data.

One of the calibration results on different link distances is shown in Figure 11. For each link distance, no matter the object is on MPL or on MVL, the RSSI dynamics grow higher when the object moves closer to its midpoint. Therefore, for each dynamic line on MPL and MVL, we use a threshold to intercept it. We denote the interval on MPL as the length L of the rectangle, and the interval on MVL as the width W of the rectangle. Therefore, for different influential links with the different distances, we get the size of rectangles and complete the calibration step.

Since we should compute the total covering area at each scanning-step and generate the rectangle for each influential link, the complexity of the best-cover algorithm is $O(nk)$, where n is the number of influential links and k is the total number of scanning times for the scanning square in the grid. The value of k depends on the side length of the grid array and the scanning step.

5. Performance Evaluation

In this section, we first describe our experimental setup and phases of the tracking system. Second, the investigation of sensor distance and dynamic threshold are given. Third, we compare the performance of the three tracking algorithms proposed in the last section. Lastly, the tests of a moving object and multiple objects are provided.

5.1. Experimental setup

We conduct experiments in an empty room with 12×9 square meters. As shown in Figure 12, since the ceiling is not level, we hang the ropes from the ceiling to set up a 4×4 sensor grid. All the sensors are 2.40 meters above the floor.

We use the popular MICA2 nodes with Chipcon CC1000 radio chips and monopole antennas [23]. Unless stated explicitly, the default transmission power is set as 0 dBm. The radio frequency is 870 MHz. We program all the sensor nodes to broadcast beacons periodically with the same interval. In order to avoid beacon collision, each node has to wait a short backoff time before broadcasting a beacon. The default beacon interval is three seconds.

Generally, all the proposed tracking algorithms consist of two phases. First, in the initialization phase, each node builds a static table to store the static RSSI values for all its neighbors after receiving enough number of beacons. The link thresholds are also computed from those static RSSI values. The initialization phase has to be carried out in the static environment. After initializing all the nodes, the system enters the tracking phase. Each node measures the RSSI dynamic value to detect the influential links. If the RSSI dynamic value on a link is higher than the corresponding link threshold, the link is considered to be an influential link and the RSSI dynamic value is reported back to the sink node. Otherwise, the dynamic value is used to update the static table.

5.2. The impact of sensor distance

In this study, we assume a rectangular 2D grid array where the distances to each of the four neighbors are the same. Clearly, the accuracy of position estimation depends on the size of the sensor grid array. Therefore, how to choose an appropriate cell size in the grid is a key point. We test the radio dynamic behavior of different sensor distances from 1m to 6m. In our experimental environment, some of the test results are shown in Figure 13.

Test results show that different sensor distances cause different RSSI dynamic behaviors. For the sensor distances, which are larger than 1m and smaller than 6m, the RSSI dynamics grow larger as the object

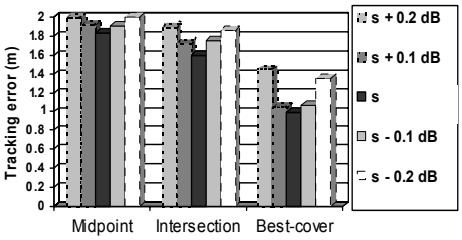

Figure 14: Test on different thresholds

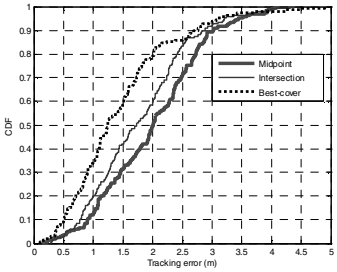

Figure 15: Algorithm comparison on all samples

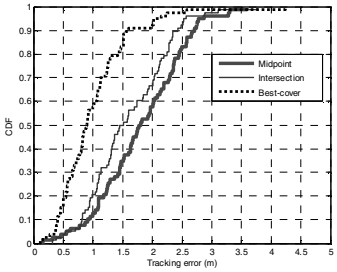

Figure 16: Algorithm comparison on non-border samples

is closer to the midpoint of MPL or MVL. We call these links *valid links*. However, for other sensor dis tances such as smaller than 1m or greater than 6m, this trend is not obvious. If the sensor distance is very short, the received signal strength is very strong on the line-of-sight radio propagation path and it is not easily influenced by the scatted wave caused by the object. On the contrary, if the sensor distance is very large, the received signal strength is very weak and is susceptible to noise interference. Therefore, we call these links as invalid links.

Among the tested valid links, we find that the dynamic behavior is the best when the sensor distance is equal to 4m. Therefore, if we set the side length between sensor nodes as 2m chosen from the candidates from 1m to 6m, the sensor grid can cover the sensor distances with 4m, 2m, and their diagonals. Thus, we can ensure the most number of valid links in our gird setting. Therefore, the best side length between sensors in the grid is 2m and we use this setting in our experiments.

Moreover, similar test of radio dynamic behavior on different sensor distances should be performed in the calibration step before running our best-cover algorithm. The invalid links can be skipped in the algorithm, so the efficiency and accuracy can be improved.

5.3. Dynamic threshold

The dynamic threshold is a key point for deciding the influential links. If its value is set very high, there are no enough influential links to localize the target objects. On the contrary, many influential links caused by noise will be taken into account, which will decrease the accuracy making a tradeoff necessary. Since noise behavior will cause some radio signal strength fluctuations in the static environment, we denote *s* as the largest difference between each measurement and the average of RSSI in the static environment. If the RSSI dynamics of a link are lower than *s*, it is likely that the RSSI dynamics are caused by noise on the link. Thus, we can eliminate the noise behaviors if we set *s* as the threshold. In order to test whether this setting is suitable, we test different thresholds above or below this empirical value. Based on 169 tested object positions, we find that no matter which algorithm we choose, the tracking errors are all larger than if we choose *s* as the threshold, as Figure 14 shows.

5.4 Comparison of algorithms

In our experiments, we test 169 sample positions in the area covered by the grid. Among these samples, there are 48 samples on the border area of the grid. We find that, whether the test samples include the border area (as shown in Figure 15) or not (as shown in Figure 16), the best-cover algorithm significantly outperforms the other two algorithms. Specifically for the non-border samples, the average tracking error of the best-cover algorithm is 0.99m. Since the total number of influential links is small when the object position is in the border area, the accuracy is not as good as it is when the object position is in the other places.

In summary, if high accuracy is not critical and with only one moving object, the intersection algorithm is a good choice as it is easy to implement and does not require calibration. Otherwise, the best-cover algorithm is recommended.

5.5. The effect of moving objects

To study the effect of a moving object, we arrange a person to walk through some fixed traces under the sensor grid. The speed of moving is 0.5 m/s. Since it is our first attempt, the speed is not very high. One of the testing traces is shown in Figure 17. The dashed line with an arrow represents the trace of the moving person. The solid line is the trace calculated by the best-cover algorithm. The average tracking error of this example is 0.74m. Another moving object example is shown in Figure 18. The average tracking of this example is 0.66m. In these two examples, when the person moves close to the border area, the number of the caused influential links is relatively small leading to the track accuracy decreasing in some extent. The latency of detecting a person in the corresponding posi-

Proceedings of the Fifth Annual IEEE International
Conference on Pervasive Computing and Communications (PerCom'07)
0-7695-2787-6/07 $20.00 © 2007 IEEE

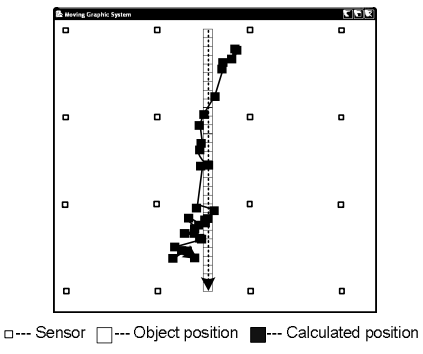

Figure 17: Moving test 1

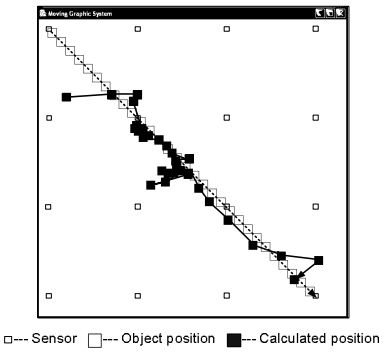

Figure 18: Moving test 2

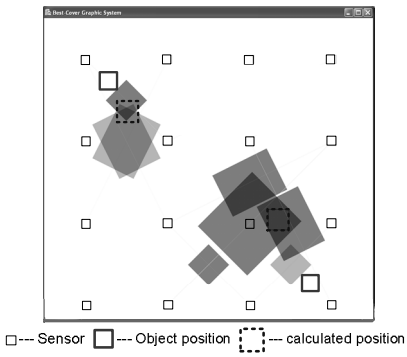

Figure 19: Multiple object test

tion is around 3 seconds, which is same as the time interval for sending beacon messages.

In summary, our system possesses the ability to catch the trace of a moving object with accuracy. However, if the object moves very fast, it is difficult for our system to catch the full trace. We can improve it by using a distributed algorithm to dynamically adjust the beacon interval. That is, if the RSSI dynamic value of one sensor is larger than the link threshold, we can decrease the beacon interval, and vice versa. Thus, we can decrease packet collisions and reduce system latency. Due to the time constraints in conducting the experiments, we leave it for our future work.

5.6. The effect of multiple objects

Detecting multiple moving objects is really a challenge for our system. With the best-cover algorithm, our system is able to recognize multiple objects by counting the number of the clusters formed by the influential links. If the objects are tightly close to each other, we regard them as one object.

An example of our experiment is shown in Figure 19, in which we have two persons. The experiment result has three disjoint clusters of rectangles. We ignore the cluster on the bottom part because it has a very small covering area. We estimate the location of the two persons based on the remaining two clusters. The tracking errors of the two persons are 1.06m and 1.86m, respectively.

6. Conclusions and Future work

We have presented three algorithms for tracking transceiver-free moving objects in WSNs. To the best of our knowledge, this is the first work to track transceiver-free objects in an indoor environment using the RF-based technology. We can maintain the properties of low cost and easy deployment while having less restriction regarding environments.

Our methods utilize the RSSI dynamic value between the static environment and the dynamic environment to calculate the target object position. Among the three algorithms, the midpoint and intersection algorithms can be used for applications without requiring high accuracy and with only one moving object. If some calibrations are performed in advance, which test the dynamic behavior and measure the possible object area by different sensor distances, the best-cover algorithm significantly beats the previous two. Furthermore, our system can also support moving object tracking. Even if there are multiple objects in our system, as long as the objects are not tightly close to each other, the best-cover algorithm is able to locate them. If the objects are tightly close to each other, we would recognize them as one object.

The algorithm complexity relies on the number of influential links. Even in a very large area covered by the sensor grid, as long as the moving objects are not crowded, the number of the influential links stays very limited. For the midpoint and intersection algorithms, the complexity is nearly constant. For the best-cover algorithm, the complexity still depends on the side length of the grid array and the scanning step.

As future work, we would like to try a larger area covered by the sensor grid. Furthermore, we may try other settings or irregular topologies instead of the grid setting to deploy sensors. For example, we may consider hexagon structure for each cell in the deployment. At each cell, the number of sensor pairs with the same distance will be larger than that in the grid setting. This may help to improve the accuracy of location estimation. Our solution to multiple moving objects is restricted. Some probabilistic models may be used to analyze the dynamic behavior of the multiple moving traces in the future.

Acknowledgements

This research was supported in part by Hong Kong RGC Grant HKUST6183/05E, the Key Project of

China NSFC Grant 60533110, the National Basic Research Program of China (973 Program) under Grant No. 2006CB303000, and the HKUST Digital Life Research Center Grant.

References

[1] ACOREL Corporation, http://www.acorel.com.

[2] Advanced Tracking Technologies, Inc., http://www.advantrack.com.

[3] P. Bahl and V. N. Padmanabhan, "RADAR: an in-building RF-based user location and tracking system," in Proceedings of the Nineteenth Annual Joint Conference of the IEEE Computer and Communications Societies, 2000.

[4] Q. Cai and J. K. Aggarwal, "Automatic tracking of human motion in indoor scenes across multiple synchronized video streams," in Proceedings of the Sixth International Conference on Computer Vision, 1998.

[5] T. Gao, D. Greenspan, M. Welsh, R. R. Juang, and A. Alm, "Vital signs monitoring and patient tracking over a wireless network," in Proceedings of the Twenty-seventh IEEE EMBS Annual International Conference, 2005.

[6] J. Jackson, "Classical electrodynamics," in 3rd ed., John Wiley & Sons Inc, 1998.

[7] J. Ma, Q. Chen, D. Zhang, and L. M. Ni, "An empirical study of radio signal strength in sensor networks using MICA2 nodes," in Technical Report, Department of Computer Science and Engineering, the Hong Kong University of Science and Technology, 2006; http://www.cse.ust.hk/~majian/papers/mica2rss_TR.pdf.

[8] M. Maróti, P. Völgyesi, S. Dóra, B. Kusý, A. Nádas, Á. Lédeczi, G. Balogh, and K. Molnár, "Radio interferometric geolocation," in Proceedings of the Third International Conference on Embedded Networked Sensor Systems, 2005.

[9] S. Meguerdichian, S. Slijepcevic, V. Karayan, and M. Potkonjak. "Localized algorithms in wireless ad-hoc networks: Location discovery and sensor exposure," in Proceedings of the Second ACM International Sympsium on Mobile Ad Hoc Networking and Computing, 2001.

[10] D. Moore, J. Leonard, D. Rus, and S. Teller, "Robust distributed network localization with noisy range measurements," in Proceedings of the Second International Conference on Embedded Networked Sensor Systems, 2004.

[11] L. M. Ni, Y. Liu, Y. C. Lau, and A. P. Patil, "LANDMARC: indoor location sensing using active RFID," in Proceedings of the First IEEE International Conference on Pervasive Computing and Communications, 2003.

[12] D. Niculescu and B. Nath. "Ad hoc positioning system (APS)," in Proceedings of IEEE Global Telecommunications Conference, 2001.

[13] D. Niculescu and B. Nath. "Ad hoc positioning system (APS) using AOA," in Proceedings of IEEE the Conference on Computer Communications, 2003.

[14] D. Pozar, "Microwave engineering," in 2nd ed., John Wiley and Sons, Inc., 1998.

[15] N. B. Priyantha, A. Chakraborty, and H. Balakrishnan, "The Cricket location-support system," in Proceedings of the Sixth Annual International Conference on Mobile Computing and Networking, 2000.

[16] T. S. Rappaport, "Wireless communications: principles and practice," in 2nd ed., Upper Saddle River, NJ: Prentice Hall PTR, 2002.

[17] J. O. Robert and D. A. Gregory, "The smart floor: a mechanism for natural user identification and tracking," in Proceedings of the CHI 2000 Conference on Human Factors in Computing Systems, 2000.

[18] Rockwell Scientific Company, http://wins.rockwellscientific. com/.

[19] R. Want, A. Hopper, V. Falcao, and J. Gibbons, "The active badge location system," in ACM Transactions on Information Systems, vol. 10, pp. 91-102, 1992.

[20] A. Woo, T. Tong, and D. Culler, "Taming the underlying challenges of reliable multihop routing in sensor networks," in Proceeding of the First International Conference on Embedded Networked Sensor Systems, 2003.

[21] G. Xu, "GPS: Theory, algorithms and applications," in Berlin: Springer-Verlag, 2003.

[22] D. B. Yang, H. H. Gonzalez-Banos, and L. J. Guibas, "Counting people in crowds with a real-time network of simple image sensors," in Proceedings of the Ninth IEEE International Conference on Computer Vision, 2003.

[23] XBOW Corporation, "XBOW MICA2 mote specifications," http://www.xbow.com.

[24] J. Yin, Q. Yang, and L. M. Ni, "Adaptive temporal radio maps for indoor location estimation," in Proceedings of the Third IEEE International Conference on Pervasive Computing and Communications, 2005.

[25] P. Zhang, C. M. Sadler, S. A. Lyon, and M. Martonosi, "Hardware design experiences in ZebraNet," in the Second ACM Conference on Embedded Networked Sensor Systems, 2004.